Available online at www.sciencedirect.com
SCIENCE DIRECT®
Journal of Hydrology 283 (2003) 91–106
Journal of Hydrology
www.elsevier.com/locate/jhydrol

A diffusive transport approach for flow routing in GIS-based flood modeling

Y.B. Liu[a,*], S. Gebremeskel[a], F. De Smedt[a], L. Hoffmann[b], L. Pfister[b]

[a]*Department of Hydrology and Hydraulic Engineering, Vrije Universieit Brussel, Pleinlaan 2, 1050 Brussels, Belgium*
[b]*Research Unit in Environment and Biotechnologies, Centre de Recherche Public-Gabriel Lippmann, Grand-Duchy, Luxembourg*

Received 11 October 2002; accepted 23 June 2003

Abstract

This paper proposes a GIS-based diffusive transport approach for the determination of rainfall runoff response and flood routing through a catchment. The watershed is represented as a grid cell mesh, and routing of runoff from each cell to the basin outlet is accomplished using the first passage time response function based on the mean and variance of the flow time distribution, which is derived from the advection–dispersion transport equation. The flow velocity is location dependent and calculated in each cell by the Manning equation based on the local slope, roughness coefficient and hydraulic radius. The hydraulic radius is determined according to the geophysical properties of the catchment and the flood frequency. The total direct runoff at the basin outlet is obtained by superimposing all contributions from every grid cell. The model is tested on the Attert catchment in Luxembourg with 30 months of observed hourly rainfall and discharge data, and the results are in excellent agreement with the measured hydrograph at the basin outlet. A sensitivity analysis shows that the parameter of flood frequency and the channel roughness coefficient have a large influence on the outflow hydrograph and the calculated watershed unit hydrograph, while the threshold of minimum slope and the threshold of drainage area in delineating channel networks have a marginal effect. Since the method accounts for spatially distributed hydrologic and geophysical characteristics of the catchment, it has great potential for studying the influence of changes in land use or soil cover on the hydrologic behavior of a river basin.

Keywords: Diffusive wave; Unit hydrograph; First passage time distribution; Geographical information system; Flood modeling

1. Introduction

In flood prediction and rainfall–runoff computation, physically based distributed modeling of watershed processes has become increasingly feasible in recent years. In addition to the development of improved computational capabilities, Digital Elevation Model (DEM), digital data of soil type and land use, as well as the tools of Geographical Information System (GIS), give new possibilities for hydrologic research in the understanding of the fundamental physical processes underlying the hydrologic cycle and of the solution of the mathematical equations representing those processes.

* Corresponding author. Tel.: +32-2-629-3335; fax: +32-2-629-3022.
E-mail addresses: yongbliu@vub.ac.be (Y.B. Liu), fdesmedt@vub.ac.be (F. De Smedt).

0022-1694/$ - see front matter © 2003 Elsevier B.V. All rights reserved.
doi:10.1016/S0022-1694(03)00242-7

Flood prediction and catchment modeling are main topics facing the hydrologist dealing with processes of transforming rainfall into a flood hydrograph and the translation of hydrographs throughout a watershed. The theory of the unit hydrograph for the prediction of stream flow in a basin has played a prominent role in hydrology for several decades since its development. This system response theory assumes that the basin response to a rainfall input is linear and time invariant. The discharge at the outlet of the basin is given by the convolution of the rainfall input and the instantaneous unit hydrograph (IUH, Dooge, 1959). In engineering practice, the unit hydrograph is often determined by numerical deconvolution techniques (Chow et al., 1988) using observed stream flow and rainfall data.

Since the characteristics of hydrologic systems, as for instance precipitation and the generation of runoff, are extremely variable in space and time, the response of the system, i.e. the flow of water over the land surface and the river channels, is a distributed process in which the characteristics of the flow change both in time and space. This limits the use of the unit hydrograph model. Consequently, in trying to relax the unit hydrograph assumptions of uniform and constant rainfall, and to account for spatial variability of the catchment, considerable research has been conducted in recent years, and many articles dealing with these topics can be found in the literature.

In an attempt to find a physical basis for the IUH, Rodriguez-Iturbe and Valdes (1979) introduced the concept of a geomorphologic instantaneous unit hydrograph (GIUH), which relates the geomorphologic structure of a basin to the IUH using probabilistic arguments. This theory was later generalized by Gupta et al. (1980) and Gupta and Waymire (1983). In their paper, Horton's empirical laws, i.e. law of stream numbers, lengths and areas, are used to describe the geomorphology of the system. The IUH is defined as the probability density function (PDF) of the droplet travel time from the source to the basin outlet, in which the time spent in each state (order of the stream in which the drop is located) is taken as a random variable with an exponential PDF. The model is relatively parsimonious in data requirements and most parameters can be obtained from DEM data. Consequently, this theory has undergone several noteworthy developments over the last two decades. Mesa and Mifflin (1986) obtained their GIUH by means of the width function and the inverse Gaussian PDF. The width function is the frequency distribution of channels with respect to flow distance from the outlet. It is an approximate representation of the 'area function' under the assumption of a uniform constant of channel maintenance throughout the drainage basin. Similar methodologies were presented by Naden (1992) and Troch et al. (1994). Sivapalan et al. (1990) incorporated the effect of partial contributing areas, which recognizes that during a rainfall event, droplets contributing to the runoff are not uniformly distributed throughout the basin but are more likely to come from areas that are saturated close to stream channels. The saturated areas can be identified through topographic indices (Beven and Kirkby, 1979), which can be easily obtained from DEM data. Van Der Tak and Bras (1990) incorporated hillslope effects in the basic formulation of GIUH by using a gamma distribution for the travel time distributions through the flow pathways and introducing a hillslope velocity term. Using the method of moments, they found that hillslope velocities are two orders of magnitude smaller than channel velocities, which has a significant impact on the GIUH. To describe the flow through individual streams, Rinaldo et al. (1991) used an advection–dispersion equation, which is obtained by introducing a diffusion term in the kinematic wave equation. They showed that not only is there a dispersion effect in the individual channels, but that the stream network structure itself causes dispersion, which is described as geomorphologic dispersion. Snell and Sivapalan (1994) showed that the geomorphologic dispersion coefficient depends on the first two moments of the flow path lengths, with the assumption of a constant flow velocity and longitudinal dispersion throughout the catchment. Lee and Yen (1997) introduced the kinematic wave theory to determine the travel times of overland and channel flows, thus relaxing the linearity restriction of the unit hydrograph theory.

Maidment (1993) proposed the promising concept of using GIS to derive a spatially distributed unit hydrograph (SDUH) that reflects the spatially distributed flow characteristics of the watershed. The SDUH is similar to GIUH, except that it uses a GIS to describe the connectivity of the links and the watershed flow network instead of probability arguments. The travel time from each cell to the watershed

outlet is calculated by dividing each flow length by a constant velocity. Subsequently, a time-area diagram based on the travel time from each grid cell is developed. A more elaborate flow model, which accounts for both translation and storage effects in the watershed, is presented by Maidment et al. (1996). In their paper, the watershed response is calculated as the sum of the responses of each individual grid cell, which is determined as a combined process of channel flow followed by a linear reservoir routing. Olivera and Maidment (1999) proposed a method for routing spatially distributed excess precipitation over a watershed using response functions derived from a digital terrain model. The routing of water from one cell to the next is accomplished by using the first-passage-time response function, which is derived from the advection–dispersion equation of flow routing. The parameters of the flow path response function are related to the flow velocity and the dispersion coefficient. The watershed response is obtained as the sum of the flow path response to spatially distributed precipitation excess. De Smedt et al. (2000) proposed a flow routing method, in which the runoff is routed through the basin along flow paths determined by the topography using a diffusive wave transfer model, that enables to calculate response functions between any start and end point, depending upon slope, flow velocity and dissipation characteristics along the flow lines, and all the calculations performed with standard GIS tools.

In this paper, a diffusive transport approach for flow routing in GIS-based flood modeling is presented. A response function is determined for each grid cell depending upon two parameters, the average flow time and the variance of the flow time. The flow time and its variance are further determined by the local slope, surface roughness and the hydraulic radius. The flow path response function at the outlet of the catchment or any other downstream convergence point is calculated by convoluting the responses of all cells located within the drainage area in the form of the PDF of the first passage time distribution. This routing response serves as an instantaneous unit hydrograph and the total discharge is obtained by convolution of the flow response from all spatially distributed precipitation excess. The model is applied to the Attert basin in the Grand-duchy of Luxembourg, for which topography and soil data are available in GIS form, and land use data is obtained from remote sensed images. River discharges are estimated on hourly basis from October 1998 to March 2001. Consequently, a sensitivity analysis is conducted to study the effect on the IUH and the predicted hydrograph at the basin outlet such as the hydraulic radius, the channel roughness coefficient, the threshold of minimum slope, and the area threshold of delineating permanent channel networks. The parameters, which significantly affect the IUH and the general applicability of the model, are also discussed.

2. Methodology

Starting from the continuity equation and the St Venant momentum equation, assuming one-dimensional unsteady flow, and neglecting the inertial terms and the lateral inflow to the flow element, the flow process can be modeled by the diffusive wave equation (Cunge et al., 1980):

$$\frac{\partial Q}{\partial t} + c\frac{\partial Q}{\partial x} - D\frac{\partial^2 Q}{\partial x^2} = 0 \tag{1}$$

Where Q [L^3T^{-1}] is the discharge at time t and location x, t [T] is the time, x [L] is the distance along the flow direction, c [LT^{-1}] is the kinematic wave celerity and is interpreted as the velocity by which a disturbance travels along the flow path, and D [L^2T^{-1}] is the dispersion coefficient, which measures the tendency of the disturbance to disperse longitudinally as it travels downstream. Such dispersion is induced by turbulence initiated from the shearing effects of channel boundaries (Mesa and Mifflin, 1986; Rinaldo et al., 1991). Assuming that the bottom slope remains constant and the hydraulic radius approaches the average flow depth for overland flow and watercourses, c and D can be estimated using the relation of Manning, by $c = (5/3)v$, and $D = (vR)/(2S)$ (Henderson, 1966), where v is the flow velocity, R the hydraulic radius and S the bed slope. Parameters c and D are assumed to be independent of the discharge, Q. Hence, the partial differential Eq. (1) becomes parabolic, having only one dependent variable, Q (x, t).

Considering a system bounded by a transmitting barrier upstream and an adsorbing barrier

downstream, the solution of Eq. (1) at the cell outlet with cell size of l [L], can be obtained using Laplace transforms for a unit impulse input (Eagleson, 1970), which results in a PDF of the first passage time distribution

$$u(t) = \frac{l}{2\sqrt{\pi D t^3}} \exp\left[-\frac{(ct - l)^2}{4Dt} \right] \tag{2}$$

where $u(t)$ [T^{-1}] is the cell response function, and is equal to the PDF of the travel time spent in a flow element, X [T], which is considered to be a random variable independent of those in the other flow elements. From a physical point of view, the independence of flow elements implies that the travel time a water particle spends in a grid cell is not related to the time spent in any other cells, and the transport dynamics depend solely on local variables and parameters and not on the conditions in the surrounding cells (Maidment et al., 1996). Consequently, the first three moments can be derived from the moment generating function of the first passage time distribution (De Groot, 1986, p. 201) as $E(X) = l/c$, $\mathrm{Var}(X) = 2Dl/c^3$, $\mathrm{Skw}(X) = 12D^2 l/c^5$, where $E(X)$, $\mathrm{Var}(X)$ and $\mathrm{Skw}(X)$ are the mean, variance and skewness of the random variable X.

Since the total time spent in the flow path, Y [T], is equal to the sum of the times spent in each of its components along the flow path, Y is also a random variable independent of those in the other flow paths. In probability theory, the PDF of the sum of a finite number of random variables is defined as the sequential convolution of their PDFs. Therefore, the flow path redistribution function, which is equal to the PDF of the random variable Y, can be obtained through the sequential convolution of the PDF's of the random variable X within the flow path. Mathematically, this convolution can be performed only by numerical integration and therefore has no analytical representation (Olivera and Maidment, 1999). For a flow path consisting of N elements, $N - 1$ convolutions have to be performed in order to get the flow path redistribution function. Furthermore, this process has to be worked out for each flow path in the watershed. Due to the enormous amount of calculations that have to be performed, the method of numerical integration is not feasible and difficult to realize in the hydrologic models. Hence, an approximate numerical solution is preferable in finding the PDF of Y, given that the PDFs of all X in the flow path are known. Although it is not possible to obtain an exact solution to the sequential convolution, the moments of the sequential convolution can be determined using the probability theory. De Groot (1986, p. 188, 197), proves that the expected value and the variance of the sum of the random variables are equal to the sum of their expected values and variances. For a first passage time distribution, the equations can be expressed as

$$E(Y) = t_0 = \int \frac{1}{c} \mathrm{d}x \tag{3}$$

$$\mathrm{Var}(Y) = \sigma^2 = 2 \int \frac{D}{c^3} \mathrm{d}x \tag{4}$$

where t_0 [T] is the average travel time from the cell to the basin outlet along the flow path, and σ^2 [T^2] is the variance of the flow time. Likewise, it can be proven that the skewness of the sum of the independent variables is equal to the sum of their skewnesses

$$\mathrm{Skw}(Y) = 12 \int \frac{D^2}{c^5} \mathrm{d}x \tag{5}$$

An approximate solution of the flow path response function is then obtained in the form of a first passage time distribution, which satisfies the statistical requirement of the first three moments as described above. The equation is written as

$$U(t) = \frac{1}{\sigma\sqrt{2\pi t^3/t_0^3}} \exp\left[-\frac{(t - t_0)^2}{2\sigma^2 t/t_0} \right] \tag{6}$$

where $U(t)$ [T^{-1}] is the flow path unit response function, and σ [T] is the standard deviation of the flow time. The parameters t_0 and σ in Eq. (6) are spatially distributed, so that each flow path has different parameters depending on the length of the flow path and the physical characteristics of the flow path elements. From a hydraulic point of view, Eq. (6) describes an elementary wave serving as an IUH of the flow path. Examples of such IUH at the end of the flow path are presented in Fig. 1a and b as a function of time. It is seen that the IUH is asymmetric with respect to time caused by the wave attenuation.

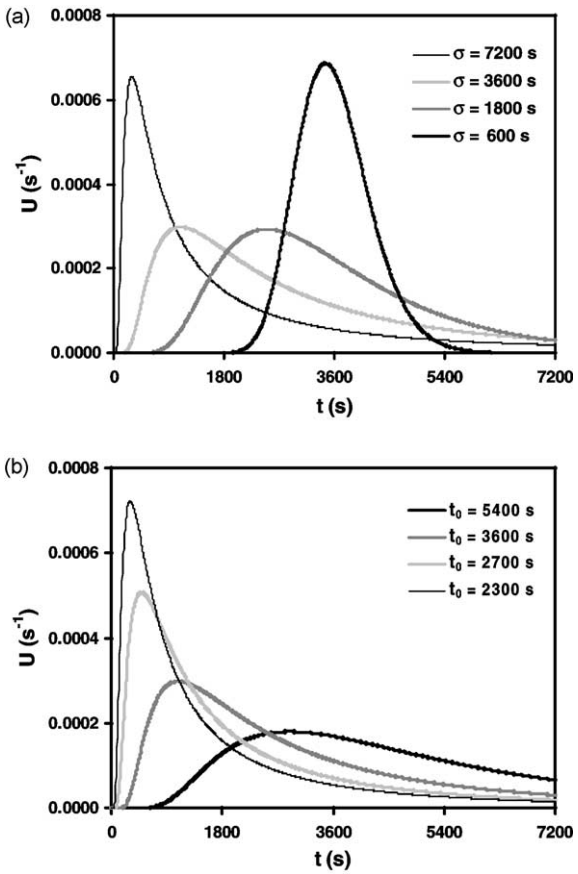

Fig. 1. (a) Unit response function for an expected travel time of 3600 s and different standard deviations, and (b) Unit response function for an expected standard deviation of 3600 s and different travel times.

Fig. 1a and b show that the approximate solution of the diffusive wave equation satisfies the general characteristics of longitudinal wave dispersion along a flow path, i.e. for a given variance of the flow time, more travel time results in less wave attenuation, and for a given average travel time, more variance of the flow time results in more wave attenuation. When σ^2 is small, the IUH tends to a normal distribution and the wave propagates as a pure translation in the limit $\sigma^2 \rightarrow 0$. Olivera and Maidment (1999) compare the goodness of the approximation of three probability distributions: normal, gamma and first-passage-time, with the exact numerical integral solution of the sequential convolution. They conclude that no statistical reasons make one function better than the others. The first passage time distribution is chosen in this study, because the two parameters t_0 and σ^2 are physically based and can be estimated conveniently by using standard GIS functions, e.g. Eqs. (3) and (4) can be calculated with the weighted flow length function, included in all commercially available GIS software that operates on raster data. Moreover, the first passage time distribution has been used other studies (Mesa and Mifflin, 1986; Naden, 1992; Troch et al., 1994; Olivera and Maidment, 1999) for modeling the time spent by water in hydrologic systems. The total flow hydrograph at the basin outlet can be obtained by a convolution integral of the flow response from all grid cells.

$$Q(t) = \int_A \int_0^t I(\tau)U(t-\tau)\mathrm{d}\tau\,\mathrm{d}A \tag{7}$$

where $Q(t)$ [L^3T^{-1}] is the outlet flow hydrograph, $I(t)$ [LT^{-1}] is the excess precipitation in a grid cell, τ [T] is the time delay and A [L^2] is the drainage area of the watershed.

For the purpose of model parameter optimization and sensitivity analysis, a watershed unit response function is proposed in this paper based on the flow path redistribution function described above. The watershed IUH differs from the traditional GIUH, which uses the drainage basin hillslope function weighted by the channel network width function (Troch et al., 1994), because it integrates the flow path response functions in the basin weighted by the spatially distributed runoff coefficient

$$UH(t) = \frac{\int_A CU(t)\mathrm{d}A}{\int_A C\mathrm{d}A} \tag{8}$$

where $UH(t)$ [T^{-1}] is the IUH of the catchment or subcatchment, and C [−] is the default runoff coefficient of the grid cell, which is assumed to depend upon slope, soil type and land use. Values of the default runoff coefficient can be collected from the literature (Kirkby, 1978; Chow et al., 1988; Browne, 1990; Mallants and Feyen, 1990; Pilgrim and Cordery, 1993). The numerator on the right hand side of Eq. (8) serves as the direct runoff hydrograph at the outlet resulting from a unit volume of rainfall but spatially distributed

surface runoff, while the denominator is the total volume of the runoff. The watershed IUH described in Eq. (8) can also be used in lumped or semi-lumped rainfall runoff models to predict outlet hydrographs with an average excess precipitation input on subcatchment or catchment scale.

3. Application

The diffusive flow routing model was tested on a subcatchment with outlet at Ell in the Attert basin, which is a main tributary of the Alzette river in the Grand-Duchy of Luxembourg (Fig. 2). The topography and soil data of the catchment are available in GIS form, and land use data was obtained from remote sensed images. The elevation in the 96.8 km^2 watershed ranges from 273 to 530 m above mean sea level, with an average basin slope of 9.6%. Fig. 3 shows the topographic elevation map of the Attert subcatchment upstream of Ell gauging station, and Fig. 4 shows the land use map of the study area. This subcatchment is partly located in Belgium and partly in the Grand-Duchy of Luxembourg. Deciduous shrub and forest are the dominant land use types of the watershed (41.1%); other land use types are agriculture (21.4%), grassland (34.1%) and urban areas (3.4%). Left-bank tributaries of the Attert are located on schistous substratum, characteristic of the Ardennes massif, whereas right-bank tributaries are located on marls and sandstone, belonging to the Paris Basin Mesozoic deposits. A very small area is covered by marshes. The dominant soil textures are loam (67.6%) and sandy loam (29.8%), while the rest is sand, loamy sand and sandy clay loam, which are scattered near the basin outlet.

The climate in the region has a northern humid oceanic regime. Rainfall is the main source of runoff and is relatively uniformly distributed over the year. High runoff occurs in winter and low runoff in summer due to the higher evapotranspiration. Winter storms are strongly influenced by the westerly atmospheric fluxes that bring humid air masses from the Atlantic Ocean (Pfister et al., 2000), and floods happen frequently because of saturated soils and low

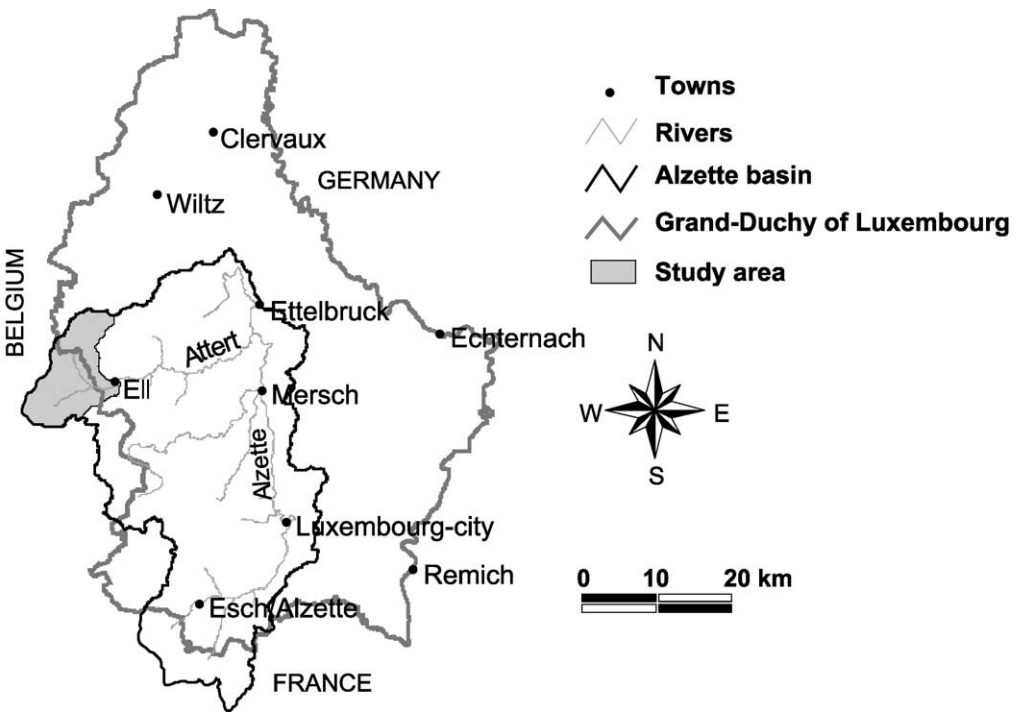

Fig. 2. Location plan showing the study area, the Attert and Alzette river basin.

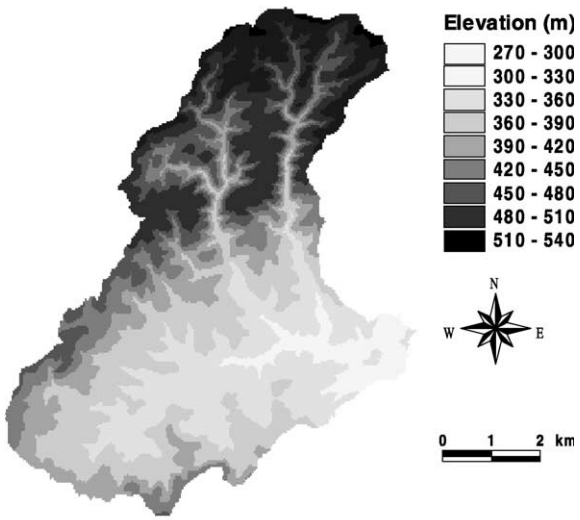

Fig. 3. DEM of the study area.

evapotranspiration. The average annual precipitation in the region varies between 800 and 1000 mm, and the annual potential evapotranspiration is around 570 mm. Precipitation generally exceeds potential evapotranspiration except for four months in summer. A total of 30 months of hourly precipitation, discharge and potential evapotranspiration data are available at Ell station. The average flow during the monitoring period is 2.41 m^3/s, with flows ranging from 0.4 to 29.8 m^3/s.

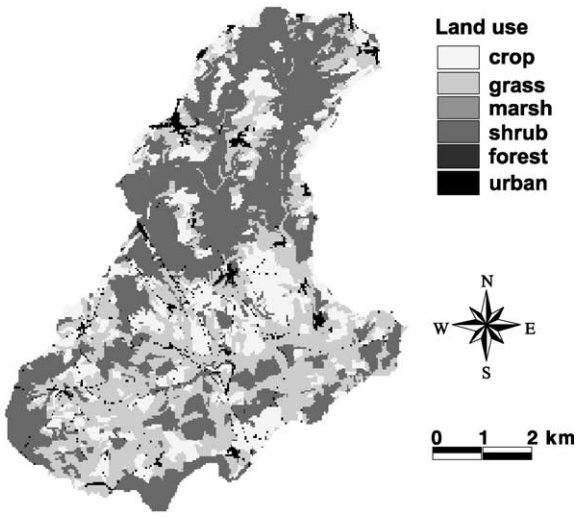

Fig. 4. Land use map of the study area.

Model parameters are identified using GIS tools and lookup tables, which relate default model parameters to the base maps, or a combination of the base maps. Starting from the 50 by 50 m^2 pixel resolution digital elevation map, hydrologic features including surface slope, flow direction, flow accumulation, flow length, stream network, drainage area and sub-basins are delineated. The threshold for delineating the stream network is set to 10, i.e. the cell is considered to be drained by ditches or streams when the total drained area becomes greater than 25,000 m^2. A map of Manning's roughness coefficients is derived from the land use map, and a map of potential runoff coefficients is calculated from the slope, soil type and land use class combinations (Liu et al., 2002). Impervious areas have significant influence on the runoff production in a watershed, because these can generate direct runoff even during small storms. Due to the model 50 m grid size, cells may not be 100% impervious in reality. In this study, the percentage of impervious area in a grid cell is computed based on land use classes, with 30% for residential area, 70% for commercial and industrial area and 100% for streams, lakes and bare exposed rock. Default potential runoff coefficients for these areas are calculated by adding the impervious percentage with a grass runoff coefficient multiplied by the remaining area. This results in runoff coefficients of 40–100% in urban areas, while other areas have much smaller values, down to 5% for forests in valleys with practically zero slopes. The map of the potential runoff coefficient of the study area is given in Fig. 5.

For calculation of the spatially distributed flow velocity and dispersion coefficient, both parameters are assumed to depend on local slope, hydraulic radius and vegetation type. This differs from previous work, where the flow velocity and dispersion coefficient are considered to be uniform distributed over the hillslope and the channel networks and estimated by model calibration (Van Der Tak and Bras, 1990; Troch et al., 1994; Gyasi-Agyei et al., 1996; Olivera and Maidment, 1999). In this study, the roughness coefficients for river courses and different land uses are obtained from literature (Chow, 1964; Yen, 1991; Ferguson, 1998), while the hydraulic radius is determined by a power law relationship with an exceeding probability

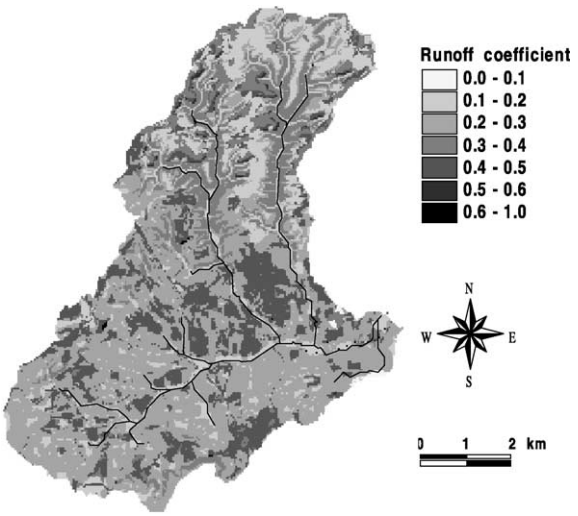

Fig. 5. Distribution of potential runoff coefficient.

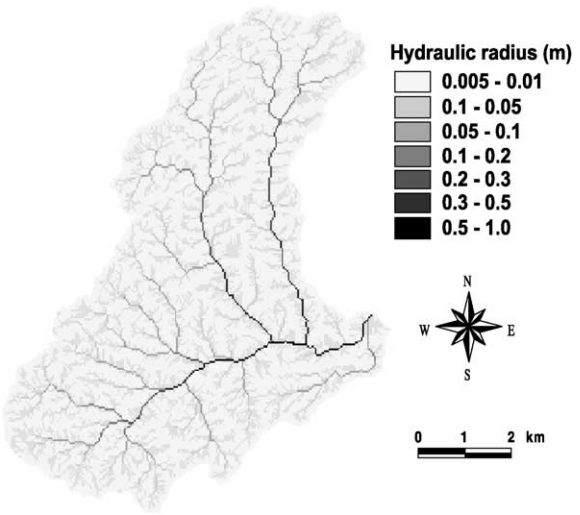

Fig. 6. Distribution of hydraulic radius for a flood with a 2-year return period.

(Molnar and Ramirez, 1998), which relates hydraulic radius to the drained area and is seen as a representation of the average behavior of the cell and the channel geometry, i.e.

$$R_p = a(A_d)^b \tag{9}$$

Where R_p [L] is the hydraulic radius with exceeding probability p, A_d [L^2] is the drained area upstream of the cell, which can be easily determined by the flow accumulation routine in standard GIS, a [−] is a network constant and b [−] a geometry scaling exponent both depending on the discharge frequency. In determining the parameters a and b for a fixed flood frequency, the minimum and maximum hydraulic radius, corresponding to a drained area of a single cell and the whole catchment, are determined firstly based on basin characteristics or estimated when catchment geohydrologic data is available. By substituting these values into Eq. (9), a and b can be determined. Consequently, the hydraulic radius for each grid cell in the basin is calculated with Eq. (9). In this study, the exceeding probability p is set to a 2-year return period for normal floods with corresponding a and b values of 0.10 and 0.50. This causes the minimum hydraulic radius for overland flow to be 0.005 m and the maximum hydraulic radius for channel flow 1 m at the basin outlet. The values of a and b can be increased for more extreme floods. Fig. 6 shows the spatial distribution of the hydraulic radius for a flood with a 2-year return period.

Because the local slope in some cells derived from the DEM can be very small and even can reach zero particularly in the river valleys in the flood plain area, the calculated flow time and its variance become very large and the computed flow path IUH is unrealistic. Therefore, a threshold for the minimum slope should be fixed, in order to make the flow path IUH more reasonable. In this study, the threshold of the minimum slope is set to 0.05%, i.e. the local slope is considered to be at least 0.05%. Thereafter, by combining the maps of the hydraulic radius, Manning's roughness coefficient, and surface slope, the average flow velocity in each grid cell can be calculated using Manning's equation, which results in velocities in the order of 0.005 m/s for overland flow on upland areas in the watershed, and up to 2 m/s for some parts of the main river. The contributing area is then determined from topographic data for a particular downstream convergence point, normally the cells corresponding to the main river or the basin outlet. Fig. 7a shows the spatial distribution of the average flow time to the basin outlet from each grid cell, and Fig. 7b shows the spatial distribution of the standard deviation of the flow time. The average flow time is less than 4 h for the main river and up to 15 h for the most remote areas, and the standard deviation

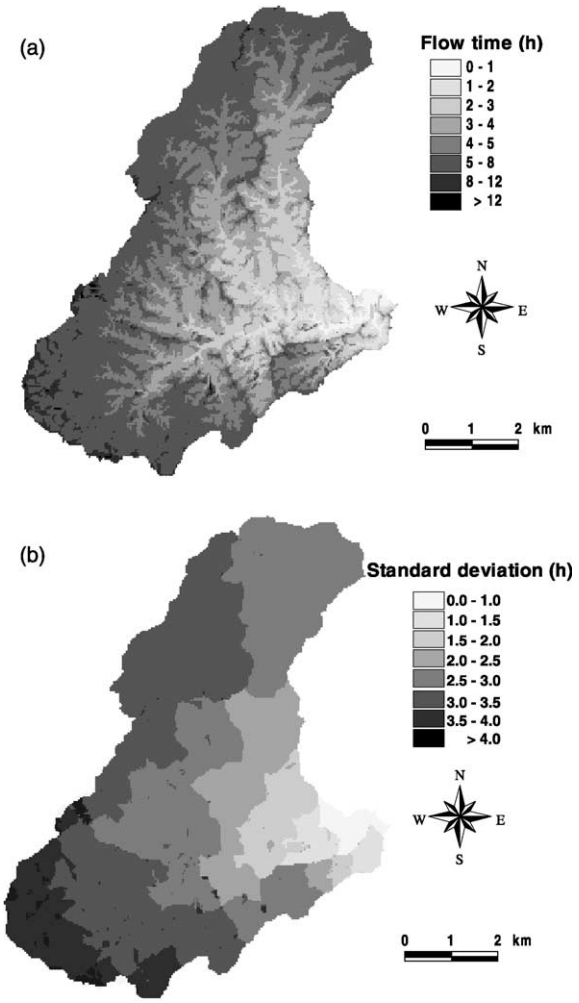

Fig. 7. (a) Average flow time to the basin outlet and (b) its standard deviation.

increases with flow length up to 5 h for the most remote cells. With the above information, the flow path unit response functions are calculated for each grid cell to the basin outlet using Eq. (6), and the watershed unit response function can be calculated using Eq. (8), weighted by the spatially distributed runoff coefficient. The calculated watershed IUH is shown in Fig. 10b.

The generation of surface runoff is performed using the WetSpa (Water and Energy Transfer between Soil, Plants and Atmosphere) model developed by Wang et al. (1996), De Smedt et al. (2000) and Liu et al. (2002), in which the runoff production in the cell is calculated by the method of default runoff coefficients and controlled by the rainfall intensity and the soil moisture content. A linear relationship is assumed between the actual surface runoff and the soil moisture content in the root zone, where wet soils tend to generate more runoff and dry soils tend to generate less or even no runoff. The soil moisture content in each cell is further simulated on the basis of a soil water balance on hourly time scale, which relies on the rate of the infiltration, percolation, interflow and evapotranspiration in and out of the root zone. Finally, the hydrograph at the basin outlet is obtained by the convolution integral of the excess precipitation and the flow path IUH from all cells in the watershed with Eq. (7).

In order to evaluate the performance of the diffusive wave approximation method for the routing of surface runoff, 30 months observed hourly discharge data at the Ell station in the Attert catchment are selected for the model verification. The baseflow is separated from the total hydrograph by the nonlinear reservoir algorithm (Wittenberg and Sivapalan, 1999), in which the baseflow is assumed to be proportional to the square of the groundwater storage as

$$Q_g = kS^2 \tag{10}$$

where Q_g [L^3T^{-1}] is the baseflow, S [L] is the groundwater storage, and k [LT^{-1}] is a reservoir recession coefficient, which is related to the area, shape, pore volume and transmissivity of the watershed, and can be derived from the analysis of the recession curves. Combined with the soil water balance equation, the groundwater storage can be determined and used for baseflow separation with Eq. (10). It turns out that the computed surface runoff hydrographs compared very well with the observations. As a typical example, we show the results for a flood event that occurred from October 23 to November 13, 1998, shown in Fig. 8, where the baseflow volume takes about 69% of the total flood volume, and the direct flow about 31%. The diffusive flow routing model is then applied with spatially distributed excess rainfall as input and the hydrograph at the basin outlet as output.

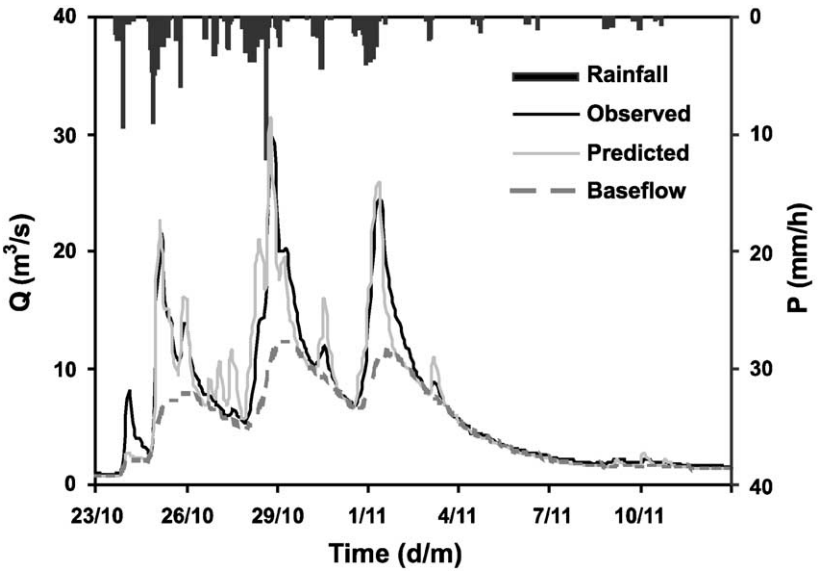

Fig. 8. Observed and predicted stream flow and baseflow separation at Ell station.

The predicted direct flow plus baseflow versus observed hydrograph is shown in Fig. 8 for the same period. The maximum recorded rainfall intensity during this period is 12 mm/h, yielding an observed peak discharge of 29.8 m^3/s, while the simulated peak flow is 31.4 m^3/s. As can be seen in the figure, the predicted hydrograph is in good agreement with the observations.

The results for other periods of the 30 months observation series are similar. A scatter plot of observed versus simulated peak direct discharges of the 24 largest storm events that occurred during the 30 months simulation period are presented in Fig. 9, in which the measured peak direct discharge is given as the observed peak discharge minus the baseflow. As can be seen in the figure, peak floods are reproduced fairly well, while the low floods tend to be somewhat overestimated by the model. This is because the frequency used to estimate the hydraulic radius in the model is a 2-year return period, which may not be correct for simulating more frequent flood events. For assessing the model performance, three evaluation criteria were applied to the simulation results for the whole simulation period: (1) the model reproduces the volume of surface runoff with 8% under estimation, (2) the model Nash–Sutcliffe efficiency (Nash and Sutcliffe, 1970) for reproducing the direct discharges is 83%, and (3) the average correlation coefficient between the measured and predicted hydrograph is 76%. Also, the prediction errors of the time to the peak of the 24 flood events are within 3 h, which

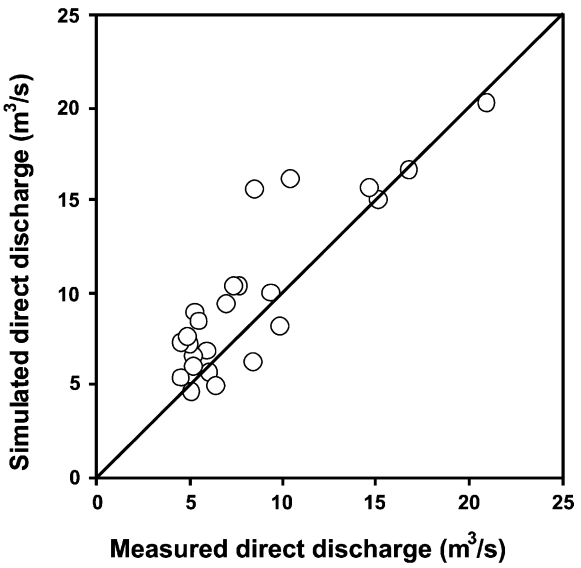

Fig. 9. Measured vs. simulated peak direct discharge for a storm event.

proves that the diffusive transport model is very well suited for flood prediction in the Attert basin.

4. Sensitivity analysis

The basic purpose of the sensitivity analysis is to determine differences in the model responses as a result of changes in the values of specific parameters. In the present study, a sensitivity analysis was conducted for the hydraulic radius, the channel roughness coefficient, the threshold for minimum slope, and the area threshold in delineating channel networks. The sensitivity results are, however, site specific and may vary with locations of different catchment size, soils, land use, and slope configurations. The effect of each parameter is studied by varying its value while keeping other parameters constant. In all cases, the predicted hydrograph for a flood event in October 1998 is considered as references. The calculated watershed IUH by Eq. (8) is also presented to give a graphical view of the effect on the mean, variance and skewness of the average travel time, even though it is not used to calculate the outlet hydrograph.

4.1. Effect of hydraulic radius

Instead of using a constant hillslope velocity and channel flow velocity to calculate the flow path response and watershed response as in many of the previous works, the concept of minimum energy expenditure is applied here to derive the hydraulic radius. The flow velocity is considered to be location dependent relying on the roughness coefficient, the local slope, and the hydraulic radius. The average hydraulic radius is obtained by the power law relationship given by Eq. (9) (Molnar and Ramirez, 1998), which is assumed to be constant for a flood event, but may vary from event to event according to the flood frequency.

Three flood frequencies, namely 0.1, 0.5 and 2.0, were considered to study their influence on the runoff hydrograph at the outlet and the watershed IUH, while keeping other parameters constant. The frequencies, 0.1, 0.5 and 2.0, correspond to return periods of 10, 2 and 0.5 years, respectively. The corresponding values of calculated hydraulic radius at the basin outlet are about 1.5, 1.0 and 0.5 m, respectively, while the minimum value of the hydraulic radius remain constant at 5 mm for surface runoff in the upstream part of the catchment. It is found from Fig. 10a that a change in the flood frequency causes a considerable alteration in the peak value of the simulated direct hydrographs and the catchment IUH. The peak discharge increases from 16.7 to 17.8 m^3/s and shifts 1 h ahead as the flood frequency decreases from 0.5 to 0.1, and decreases to 14.7 m^3/s with 1 h time delay as the flood frequency increases to 2.0. This is logical because big storms lead to higher peak discharges and shorter travel times. Fig. 10b shows the effect of the hydraulic radius on the calculated watershed IUH. The mean, variance and the skewness of the travel

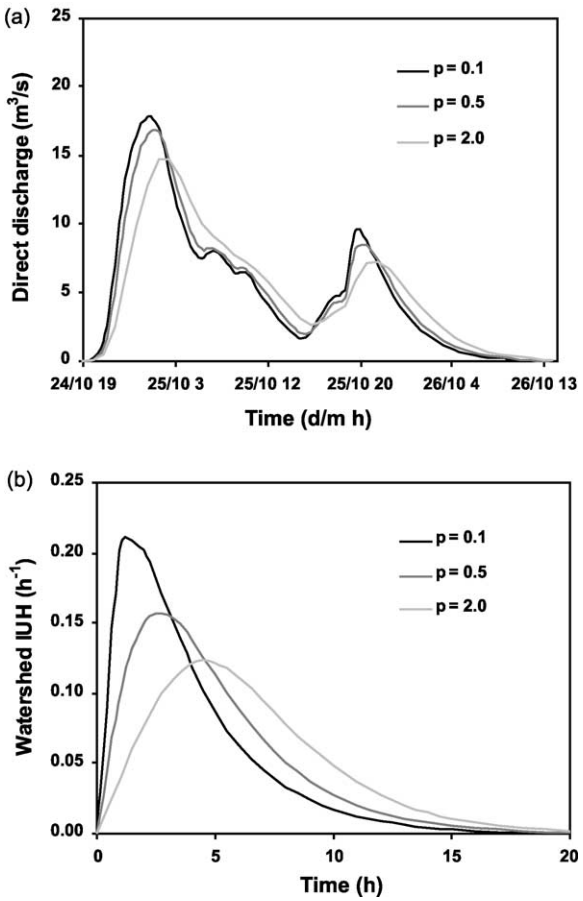

Fig. 10. (a) Simulated direct hydrographs and (b) calculated watershed IUH showing the effect of hydraulic radius with expected frequency, *p*.

time are decreasing with increased flood frequency, because these parameters are inversely depending on the celerity, as can be seen from Eqs. (3)–(5), and any increase in hydraulic radius will result in less damping and faster response of the flood wave.

4.2. Effect of channel roughness

Since surface runoff from each grid cell will contribute to the stream flow, the roughness coefficient has a direct impact on the travel time and amount of dissipation that will occur when routing a flood hydrograph through a river basin. Roughness coefficients for hydrologic routing models are typically in the form of Manning's n values, and estimated based on the channel geometry. Generally, the roughness coefficient is higher for upstream channels, and decreases with stream order when the channel slope becomes small. For the convenience of model computation and result comparison, the channel roughness coefficient is considered to be constant in this example regardless of the effect of stream order. Fig. 11a shows the simulated direct runoff hydrographs and the calculated watershed IUH with three different values of Manning's roughness coefficient. The value 0.03 corresponds to clean and straight streams without riffles or deep pools, 0.04 to clean and winding streams with some pools and shoals, and 0.05 to clean and winding streams with stones (Chow, 1964). It is found that the peak discharge decreases from 16.7 to 14.3 m^3/s and is somewhat delayed as the roughness coefficient increases from 0.04 to 0.05, and increases to 20.2 m^3/s with 1 h shifting ahead as the roughness coefficient decreases to 0.03. Since the total runoff volume remains constant, reduction in peak discharge and delay in peak time are compensated by prolonged flow recession, and vice versa. This is also reflected in the calculated watershed IUH as shown in Fig. 11b. The mean, variance and the skewness of the travel time are increasing with increasing roughness, due to the fact that any increase in roughness coefficient will result in higher shear stresses, causing more damping and slowing down of the flood wave.

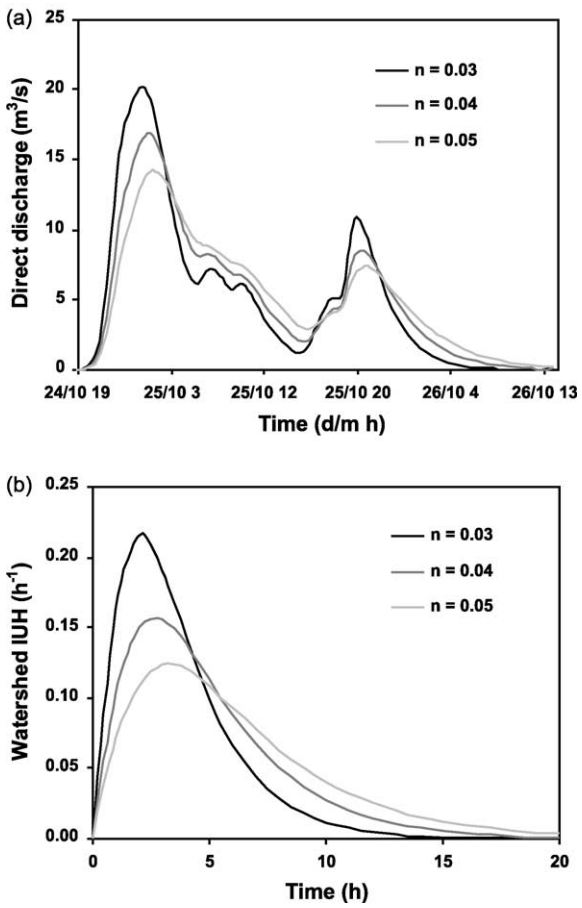

Fig. 11. (a) Simulated direct hydrographs and (b) calculated watershed IUH showing the effect of channel Manning's roughness coefficient, n.

4.3. Effect of minimum slope

The present approach considers the changes in velocity with respect to distance, but ignores the changes in velocity with respect to time. Therefore, it can be used to route slow rising floodwaves through very flat slopes, but errors in the amount of damping will occur when routing rapidly rising flood waves through extremely flat channel slopes, because the inertia terms are not included in the diffusion wave method. In GIS, the slope of the cell is derived from the DEM and calculated from the 3×3 neighbourhood using the average maximum technique. Inevitably, nearly zero slopes may occur in some areas, especially in the river valleys in the flood plain area, resulting in nearly infinity travel time and damping. To mitigate the impact of the extremely flat slopes on the flow path function, it is necessary to import

a threshold for minimum slope, i.e. the cell slope is put equal to the threshold value when the calculated slope is smaller than the threshold.

Keeping all other parameters constant, three values of minimum slope, namely, 0.01, 0.05 and 0.1% are considered to study the effect of the threshold value on the outflow hydrograph and the calculated watershed IUH. Results are shown in Fig. 12a and b. It is found that the peak discharge and the time to the peak of the watershed IUH decrease slightly with a smaller threshold for minimum slope. This is because a decrease in slope will reduce the flood wave celerity, and therefore increase the travel time and the amount of hydrograph attenuation. Since the number of cells with a slope lower that the thresholds is small in this catchment, the influence of the minimum slope is not very significant as can be seen in the figure. However, the minimum slope may have a large influence on the outflow hydrograph for catchments with flatter slopes.

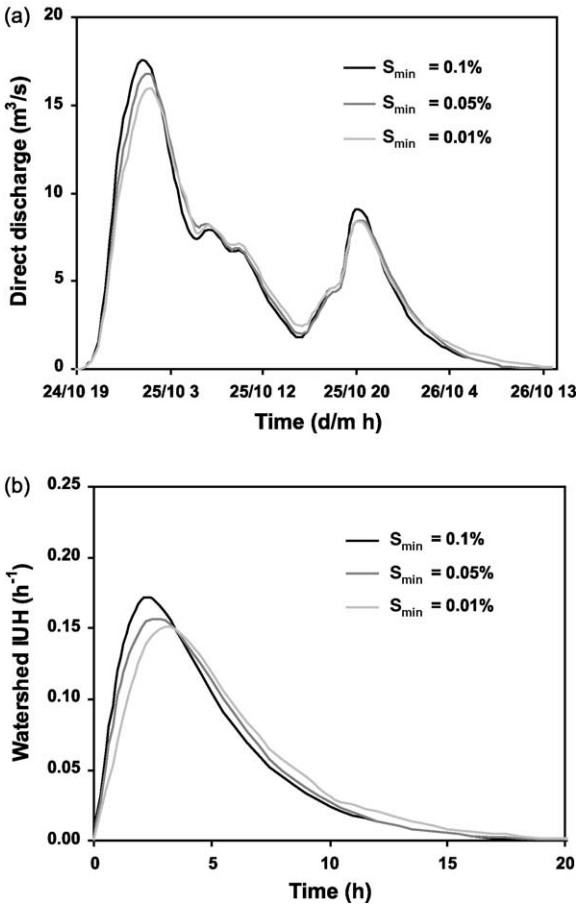

Fig. 12. (a) Simulated direct hydrographs and (b) calculated watershed IUH showing the effect of the threshold of minimum slope, S_{min}.

4.4. Effect of area threshold in delineating channel networks

In standard GIS applications, such as ArcInfo and ArcView, watershed channels are delineated based on the upstream area of each cell. It is assumed that any upstream area smaller than the threshold value does not produce enough runoff to support a channel. The area required to develop a channel depends on regional and watershed characteristics such as climatic conditions, soil properties, surface cover, and slope characteristics (Martz and Garbrecht, 1992). In cells that are not part of the stream network, overland flow occurs. Therefore, with a small area threshold value, GIS derived stream networks are more meticulous and may represent ephemeral and intermittent streams that are too small to be represented on topographical maps.

The effect of the area threshold in delineating channel networks on the outflow hydrograph and the calculated watershed IUH is investigated by varying the cell number threshold, namely 5, 10 and 50, which corresponds to draining areas of, respectively, 12,500, 25,000 and 125,000 m^2, while keeping other model parameters constant. It can be seen from Fig. 13a and b, that there is no significant effect on the peak discharge and the calculated watershed IUH in this catchment. This is due to the fact that changes in the threshold area will result in expansion or shrinking of the stream network with lengths that are, however, relatively short compared to the whole flow paths. Hence, the impact will only become significant when using large threshold values, because in this case hillslope effects become important due to their high overland flow roughness, which will result in a longer flow time, and a prolonged flow response at the end of the flow path.

4.5. Other effects

In addition to the effects discussed above, the variation of channel geometry and the temporal and

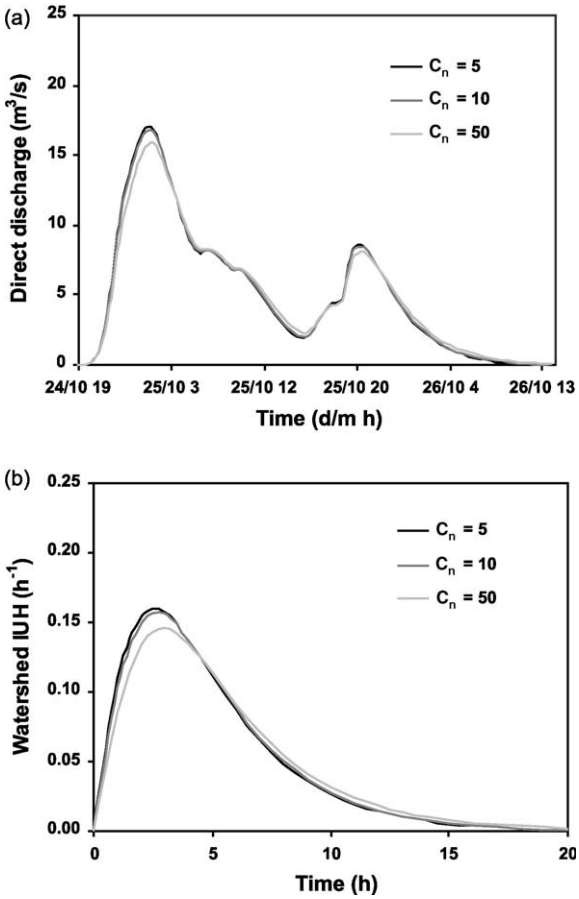

Fig. 13. (a) Simulated direct hydrographs and (b) calculated watershed IUH showing the effect of area threshold in delineating channel networks with cell number threshold, C_n.

spatial resolutions of the model will also have considerable influence on the outflow hydrograph and the watershed IUH. In this study, flow is routed using a velocity calculated for each land use category both for overland flow and channel flow. The velocity is determined from Manning's equation by assuming that the hydraulic radius equals the average flow depth without considering the effect of channel width and type. This assumption is warranted if the width of the river is much larger than its depth for a flood event. However, as the width of a channel decreases, the hydraulic radius does not tend towards the average flow depth. Also, the effect of flood plains on the propagation of a floodwave can be very significant, when water overflows the riverbanks. It is expected that an expanded channel width will slow down the flow velocity and therefore reduce the peak discharge and delay the resulting runoff hydrograph. Hence, more reliable results can be obtained when calculating the hydraulic radius combined with measured or estimated channel width.

The time and space scale of the model not only influence on rainfall intensity and the surface runoff distribution, but they also have impacts on the watershed IUH derived from the diffusive transport method. Errors may arise when modeling flash flood for a small catchment with a long time scale. This is because floodwater can flow out of the catchment within the first time step, which the IUH cannot calculate accordingly. Therefore, a lower time resolution is necessary in this case. However, when modeling floods in a large catchment with relatively long concentration times, the effect of time scale is not important. On the other hand, changes in spatial resolution of the model will lead to variations of the GIS derived slope, flow direction, and spatial distribution of the flow paths. In general, higher spatial resolution tends to generate longer flow paths, and hence increases the hydrodynamic and the geomorphologic attenuation of the flood wave. The first is due to increased flow time, and the second to increased variability of the flow paths. Both impacts will play an important role in the prediction of transport phenomena, especially in large basins (Rinaldo et al., 1991). It is expected that reduction in the spatial resolution will result in a decrease of peak discharge and prolonged time to flood peaks, and vice versa.

As pointed out by Horritt and Bates (2001), a high-resolution model is advantageous when small scale processes have a significant effect on model predictions, but have to be balanced against the increased computation onus. Predictions with a low-resolution may also give an essentially correct result in many cases. In practice, determination of temporal and spatial resolution of the model should rely on the data available, the catchment characteristics and the model accuracy requirement. However, quantitative analysis of these effects on the outflow hydrograph and the watershed IUH in GIS flood modeling is beyond the scope of this paper.

5. Conclusions

A physically based distributed unit hydrograph method derived from the diffusive transport approach is presented in this paper for GIS based modeling on catchment scale. The method differs from the previous work in that it is based on a location dependent velocity field. The basic modeling approach is to use raster GIS functions to calculate the travel time from each point in the watershed to the outlet by determining the flow path and the travel time through each cell along the path. The flow velocity in each grid cell is calculated by the Manning equation, which depends upon the local slope, roughness coefficient and hydraulic radius. The travel time through each individual cell along the flow path is integrated to obtain the cumulative travel time to the outlet. Based on the mean and the variance of the flow time, the first passage time distribution density function is applied as a flow response function. Runoff is routed over the surface flow path, and accounts for the differences in runoff amount and velocity, due to changing slope, land use, soil type and other surface conditions. Finally, the total direct discharge at the downstream convergence point is obtained by superimposing all contributions from every grid cell. The watershed IUH is calculated based on the flow path functions and the spatially distributed runoff coefficient, and can be used for model parameter sensitivity analysis or as the IUH for lumped prediction models. Model parameters based on surface slope, land use, soil type and their combinations are collected from literature, and can be prepared easily using standard GIS techniques.

The model was tested on the Attert catchment in Luxembourg with 30 months of observed hourly rainfall and discharge data, where the spatial distributed surface runoff was generated by the WetSpa model. The results show an excellent agreement with the measured hydrograph at the basin outlet. Consequently, a sensitivity analysis was conducted to study the effect of the hydraulic radius, the channel roughness coefficient, the threshold for minimum slope, and the area threshold in delineating channel networks on the outflow hydrograph and the calculated watershed IUH. It was found that the hydraulic radius and channel roughness coefficient are the most sensitive parameters. The hydraulic radius corresponding to a 2-year return period can meet the requirements of flood prediction for normal floods, but should be increased for more extreme flood. Also, the channel roughness coefficient shows a strong impact on the model output. More reliable results are expected when the channel roughness is determined according to the stream order. The thresholds of minimum slope and the area in delineating channel networks have only marginal effects on the outflow hydrograph and the calculated watershed IUH. However, all these parameters should be chosen properly when applying the model in practice.

The diffusive wave transport approach assumes a unique relationship between flow and stage at each point for both overland flow and channel flow, and so does not require the specification of a downstream stage. It also generally operates satisfactorily with less detailed ditch and channel geometry information than required by dynamic wave models and is much more stable and easy to use in GIS based flood modeling. Moreover, this approach allows the spatially distributed excess precipitation and hydrologic parameters of the terrain to be used as inputs to the model, and is especially useful to analyze the effects of topography, and land use or soil cover on the hydrologic behavior of a river basin. The method is worth to be applied in flood modeling for a wide range of slopes from flood plains to the hilly areas. However, accuracy of the diffusive wave approach increases with increasing slope, and it cannot be used in situations where flow reversals occur. Application of the methodology suggests that simulations of the hydrologic response based on diffusive wave approximation and GIS specification of the topographical network are validated in the study area. This is sustained by a proper adjustment of the parameter values characterizing the flow travel time and its variance, which is deemed to cover most cases of engineering interest.

References

Beven, K.J., Kirkby, M.J., 1979. A physically based variable contributing area model of basin hydrology. Hydrol. Sci. Bull. 24 (1), 43–59.

Browne, F.X., 1990. Stromewater management. In: Corbitt, R.A., (Ed.), Standard Handbook of Environmental Engineering, McGraw-Hill, New York, pp. 7.1–7.135.

Chow, V.T. (Ed.), 1964. Handbook of Applied Hydrology, McGraw-Hill Book Company, New York, pp. 7–25.

Chow, V.T., Maidment, D.R., Mays, L.W., 1988. Applied Hydrology, McGraw-Hill, New York.

Cunge, J.A., Holly, F.M., Verwey, A., 1980. Practical Aspects of Computational River Hydraulics, Pitman, London, GB, p. 45.

De Groot, M.H., 1986. Probability and Statistics, Addison-Wesley, Reading, MA, USA.

De Smedt, F., Liu, Y.B., Gebremeskel, S., 2000. Hydrologic modeling on a catchment scale using GIS and remote sensed land use information. In: Brebbia, C.A., (Ed.), Risk Analysis II, WTI press, Southampton, Boston, pp. 295–304.

Dooge, J.C.I., 1959. A general theory of the unit hydrograph. J. Geophys. Res. 64, 241–256.

Eagleson, P.S., 1970. Dynamic Hydrology, McGraw-Hill, New York, p. 364.

Ferguson, B.K., 1998. Introduction to Stormwater, Concept, Purpose and Design, Wiley, New York, p. 111.

Gupta, V.K., Waymire, E., 1983. On the formulation of an analytical approach to hydrologic response and similarity at the basin scale. J. Hydrol. 65, 95–123.

Gupta, V.K., Waymire, E., Wang, C.T., 1980. A representation of an instantaneous unit hydrograph from geomorphology. Water Resour. Res. 16 (5), 855–862.

Gyasi-Agyei, Y., De Troch, F.P., Troch, P.A., 1996. A dynamic hillslope response model in a geomorphology based rainfall–runoff model. J. Hydrol. 178, 1–18.

Henderson, F.M., 1966. Open Channel Flow, McMillan, New York, p. 522.

Horritt, M.S., Bates, P.D., 2001. Effect of spatial resolution on a raster based model of flood flow. J. Hydrol. 253, 239–2498.

Kirkby, M.J. (Ed.), 1978. Hill-slope Hydrology, Wiley, p. 235.

Lee, K.T., Yen, B.C., 1997. A geomorphology and kinematic-wave-based hydrograph derivation. J. Hydraulic Engng., ASCE 123 (1), 73–80.

Liu, Y.B., Gebremeskel, S., De Smedt, F., Pfister, L., 2002. Flood prediction with the WetSpa model on catchment scale. In: Wu, et al. (Eds.), Flood Defence'2002, Science Press, New York, pp. 499–507.

Maidment, D.R., 1993. Developing a spatially distributed unit hydrograph by using GIS. In: Dovar, K., Natchnebel, H.P. (Eds.), Application of Geographic Information Systems in Hydrology and Water Resources, Proceedings of the Vienna Conference, Vienna: Int. Assoc. of Hydrological Sci., pp. 181–192.

Maidment, D.R., Olivera, J.F., Calver, A., Eatherral, A., Fraczek, W., 1996. A unit hydrograph derived from a spatially distributed velocity field. Hydrol. Process 10 (6), 831–844.

Mallants, D., Feyen, J., 1990. Kwantitatieve en kwalitatieve aspecten van oppervlakte en grondwaterstroming (in Dutch), vol. 2. KUL, p. 96.

Martz, L.W., Garbrecht, J., 1992. Numerical definition of drainage network and subcatchment areas from digital elevation models. Comput. Geosci. 18 (6), 747–761.

Mesa, O.J., Mifflin, E.R., 1986. On the relative role of hillslope and network geometry in hydrologic response. In: Gupta, V.K., Rodriguez-Iturbe, I., Wood, E.F. (Eds.), Scale Problems in Hydrology, D. Reidel, Norwell, Mass, pp. 1–17.

Molnar, P., Ramirez, J.A., 1998. Energy dissipation theories and optimal channel characteristics of river networks. Water Resour. Res. 34 (7), 1809–1818.

Naden, P.S., 1992. spatial variability in flood estimation for large catchments: the exploitation of channel network structure. J. Hydrol. Sci. 37, 53–71.

Nash, J.E., Sutcliffe, J.V., 1970. River flow forecasting through conceptual models. J. Hydrol. 10, 282–290.

Olivera, F., Maidment, D.R., 1999. Geographic information system (GIS)-based spatially distributed model for runoff routing. Water Resour. Res. 35 (4), 1155–1164.

Pfister, L., Humbert, J., Hoffmann, L., 2000. Recent trends in rainfall–runoff characteristics in the Alzette river basin, Luxembourg. Climate Change 45 (2), 323–337.

Pilgrim, D.H., Cordery, I., 1993. Flood runoff. In: Maidment, D.R., (Ed.), Handbook of Hydrology, McGraw-Hill, New York, pp. 9.1–9.42.

Rinaldo, A., Marani, A., Rigon, R., 1991. Geomorphological dispersion. Water Resour. Res. 27 (4), 513–525.

Rodriguez-Iturbe, I., Valdes, J.B., 1979. The geomorphologic structure of hydrologic response. Water Resour. Res. 15 (6), 1409–1420.

Sivapalan, M., Wood, E.F., Beven, K., 1990. On hydrologic similarity. 3. A dimensionless flood frequency model using a generalized geomorphologic unit hydrograph and partial area runoff generation. Water Resour. Res. 26 (1), 43–58.

Snell, J.D., Sivapalan, M., 1994. On geomorphological dispersion in natural catchments and the geomorphological unit hydrograph. Water Resour. Res. 30 (7), 2311–2323.

Troch, P.A., Smith, J.A., Wood, E.F., de Troch, F.P., 1994. Hydrologic controls of large floods in a small basin. J. Hydrol. 156, 285–309.

Van Der Tak, L.D., Bras, R.L., 1990. Incorporating hillslope effects into the geomorphological instantaneous unite hydrograph. Water Resour. Res. 26 (1), 2393–2400.

Wang, Z., Batelaan, O., De Smedt, F., 1996. A distributed model for water and energy transfer between soil, plants and atmosphere (WetSpa). Phys. Chem. Earth 21 (3), 189–193.

Wittenberg, H., Sivapalan, M., 1999. Watershed groundwater balance estimation using streamflow recession analysis and baseflow separation. J. Hydrol. 219, 20–33.

Yen, B.C. (Ed.), 1991. Channel Flow Resistance: Centennial of Manning's Formula, Water Resources Publications, Littleton, CO, p. 43.